Marine Pollution Bulletin
June 2021, Volume 167 Pages 112329 (9p.)
https://doi.org/10.1016/j.marpolbul.2021.112329
https://archimer.ifremer.fr/doc/00689/80154/

Dynamic Energy Budget model suggests feeding constraints and physiological stress in black-lip pearl oysters, 5 years post mass-mortality event

Monaco Cristian [1, *], Sangare Nathanael [1, 2], Le Moullac Gilles [1], Basset Caline [1], Belliard Corinne [1], Mizuno Keiichi [3], Smith Diane L., Lo-Yat Alain [1]

[1] IFREMER, IRD, Institut Louis-Malardé, Univ Polynésie française, EIO, F-98719 Taravao, Tahiti, French Polynesia
[2] UMR 9220 ENTROPIE, Institut de Recherche Pour le Développement (IRD, Université de la Réunion, Université de la Nouvelle-Calédonie, Ifremer, CNRS), B.P.A5, 98848 Nouméa, New Caledonia
[3] IFREMER, IRD, Institut Louis-Malardé, Univ Polynésie française, EIO, F-98719 Taravao, Tahiti, French Polynesia

* Corresponding author : Cristian Monaco, email address ; cristian.monaco@ifremer.fr

Abstract :

Mass-mortality events of marine species can disturb the structure of communities. While identifying the causes of mass-mortality events is crucial for implementing recovery strategies, monitoring is challenging in remote locations. Black-lip pearl oysters (Pinctada margaritifera) are farmed for producing black pearls within remote atolls of French Polynesia. Previous mass-mortality events have resulted in the collapse of oysters and other species; however, the causes and conditions that favour recovery are unclear. We investigated the potential for oyster population recovery 5 years after a mortality event at Takaroa Atoll (Tuamotu Archipelago). Temperature, food availability (total chlorophyll-a), growth and reproduction were monitored. Growth was also simulated using a Dynamic Energy Budget model. Despite favourable conditions, reduced growth and reproduction signalled an energetic deficit. The model overpredicted growth, and supported the hypotheses that individuals are unable to profit from the phytoplankton available and maintenance costs are high in Takaroa, ultimately explaining their poor physiological condition

Highlights

► Mass-mortality events are increasingly common. ► Identifying the causes of mass-mortality events is challenging in remote locations. ► Data and an energy budget model revealed possible underlying mechanisms. ► Pearl oysters unable to profit from available phytoplankton after mass-mortality event ► Pearl oysters show high maintenance costs after mass-mortality event.

Keywords : Population collapse, Population recovery, Bivalve, Aquaculture, Tropical atoll, Energetics

1. Introduction

Mass-mortality events of marine organisms have been increasingly documented across the world, due to an intensification of both natural and anthropogenic-related stressors (Andréfouët et al., 2015; Jackson, 2008; Sarà et al., 2021; Seuront et al., 2019). Should the affected species be important ecological players and/or if they hold commercial or cultural value, the collapse of local populations can have long-lasting negative consequences (Keenan et al., 2008). For resource managers and producers, the strategies to manage the risk and impact of mass-mortality events include preventive measures (e.g., considering the natural productivity of potential rearing sites), mitigative measures (e.g., methods to reduce parasite load), and post-event measures (e.g., facilitating the recovery via translocation campaigns) (McAfee et al., 2020; Nel et al., 1996; Nielsen and Petersen, 2019).

The population collapse of many important bivalve species due to overexploitation (e.g., rock oysters globally; Beck et al., 2011) has recently led to major restoration efforts aiming to reattain baseline population densities (McAfee et al., 2020). The success of these post-event measures invariably depends on whether the *new* environmental conditions satisfy the requirements of the target species. An alternative scenario emerges when the cause of the mass mortality is unknown, for example, following microbial infections (Lallias et al., 2008; Samain and McCombie, 2008). In such cases, because the culprit might effectively linger undetected in the system long after the event, the success of restoration campaigns is often uncertain (McAfee et al., 2020). While a comprehensive characterization of the bio-physical habitat can help gauge the suitability of the *new* habitat, the practical constraints of examining every relevant variable, and the challenge of establishing cause-effect relationships calls for complementary approaches. Individual-level indicators of physiological condition, including both direct empirical observations and indirect model estimates of growth and reproduction, can help assess the potential for recovery of populations after mass-mortality events (Sawusdee et al., 2015).

The black-lip pearl oyster (*Pinctada margaritifera* Linnaeus 1758), which occurs naturally across the tropical Indian and Pacific Oceans, supports the pearl-culture industry of French Polynesia (Andréfouët et al., 2012). Farmers rely on the collection of wild oyster spats to produce pearls, but

because the activities are concentrated on a few atolls, most of which are located in the northern Tuamotu Archipelago, the production of pearls is highly susceptible to environmental stochasticity of natural and anthropogenic origin (Andréfouët et al., 2012). Since the onset of commercial pearl farming in French Polynesia in the 1970s, two major mass-mortality events of *P. margaritifera* populations have been documented in pearl-farming atolls: at Takapoto in 1985 and Takaroa in 2014, with profound knock-on effects on the livelihoods of producers and their families (Cabral, 1989; Rodier et al., 2019). At Hikueru Atoll, where no pearl farming occurs, a wholesale community-level mortality event was documented in 1994 (Adjeroud et al., 2001). Hypotheses to explain these events include the detrimental effects of microalgae blooms and microbial infections (Cabral, 1989; Harris and Fichez, 1995, Intes 1995) often associated with periods of reduced wind intensity and water exchange between the lagoon and the open ocean (Andréfouët et al., 2015), but conclusive evidence is unavailable. The historical recovery of a healthy stock of *P. margaritifera* at Takapoto within a period of five years (G Haumani [agent of the *Direction des ressources marines*], *personal communication*) suggests that the population might also recover functionally at Takaroa.

Before the 2014 collapse, the wild population at Takaroa was among the largest producers of *P. margaritifera* spats and black pearls (Andréfouët et al., 2012). Although some pearl-farming activity has been maintained after the mass-mortality event by translocating animals collected from neighbouring atolls, the productivity has remained negligible compared to previous years. There is a pressing need to determine the true potential for recovery of the wild stocks of the Takaroa Atoll. While no man-made strategies for population recovery have been implemented 5 years after the population collapse, the introduction of mature individuals for pearl farming might effectively operate as such, despite a male-biased sex ratio due to the species' protandric life cycle (Andréfouët et al. 2016; Thomas et al. 2016).

As a first approach for determining the potential for recovery of the Takaroa population of *P. margaritifera*, we investigated the suitability of environmental conditions 5 years post mass-mortality event, while explicitly considering the species' physiological requirements. Our analysis and data included (1) *in situ* time series of seawater temperature and chlorophyll-*a* (Chl-*a*, proxy for food

availability), (2) measurements of individual growth and reproduction, and (3) energy budget modelling based on the Dynamic Energy Budget (DEB) theory (Kooijman, 2010; Sangare et al. 2020; Sousa et al., 2010). The empirical data (i.e., environmental and life-history traits) allowed direct comparison of our observations against previous growth and reproduction data from neighbouring atolls, while DEB modelling provided an indirect tool to examine physiological mechanisms underlying the observed growth response. Assuming that the culprit of the mass-mortality event had receded after 5 years, we expected that suitable environmental conditions would have yielded values of growth and reproduction comparable to previous records from neighbouring atolls.

2. Materials and methods

2.1. Sampling location and environmental conditions

The Takaroa Atoll is part of the north-western Tuamotu Archipelago (French Polynesia). Our study was done at the SCA QLES pearl-farm's concession, which is centrally located along the northeast-southwest axis of the atoll, and skewed towards the wind-protected eastern boundary (14˚27'34.4" S, 144˚57'34.3" W). Takaroa is a semi-enclosed atoll with an area of 85 km², and average and maximum depths of 26 and 47.5 m, respectively (Andréfouët et al., 2020) (Fig. 1).

Between January 30th and November 6th 2019, seawater temperature and total Chl-*a* were recorded using a multiparameter sensor (NKE Smatch™) deployed at 5 m depth on a pearl-farm line. Temperature and Chl-*a* data were averaged daily for the analyses. Because measurements of Chl-*a* were subject to photoinhibition due to daylight (Charpy et al., 2012; Thomas et al., 2010), we only used nocturnal measurements taken between 18:00 and 06:00. We excluded the Chl-*a* data between 17 and 26 April because the probe was covered with fouling agents. Linear interpolation was used to fill this gap in data.

2.2. Empirical observations of growth and reproduction

We quantified the growth and reproductive potential of pearl oysters reared by a farmer in Takaroa during 2019. Animals had been previously translocated to Takaroa as spats from the neighbouring atoll of Takapoto (10 km south-west), and grown to an adult stage. Individuals were kept in standard pearl-farming cages (Netlon™, 3-cm mesh size) attached to vertical ropes suspended ~5 m deep. Cages were cleaned periodically to remove the biofouling. Animals used to examine growth were marked with plastic tags and arranged in groups of 10 individuals per cage. Individuals used to asses reproductive potential were sampled directly from the pearl-farm's stock (SCA QLES).

To quantify shell growth, we used 100 individuals measured on four dates (30/01/2019, 24/04/2019, 15/08/2019, and 06/11/2019), yielding three successive time intervals (interval 1, 84 d; interval 2: 113 d; interval 3: 84 d). On each date, we measured the dorso-ventral length using callipers (0.01-cm resolution). The initial shell length (mean ± SD) was 8.84 ± 1.14 cm (range = 7.1 – 11.5 cm). The absolute growth rate (mm d^{-1}) was calculated as the difference in shell length between successive measurements, divided by the number of days. The specific growth (% d^{-1}) was calculated by $\log_{10}$-transforming the two lengths, dividing by the number of days, and multiplying by 100 (Lugert et al., 2016). Note that growth was seemingly negative for several individuals, an artefact due to the difficulty of successively measuring the shells along exactly the same axis. We were forced to assume that this observation error was constant over time.

We examined the reproductive potential (gonad-development index) of animals collected across six months (12/02/2019 – 23/07/2019), covering an important portion of the most active reproductive period reported for *P. margaritifera* in French Polynesia (Fournier et al., 2012b). Thirty individuals were collected weekly (total = 720 individuals), transported live to the laboratory (IFREMER, *Centre du Pacifique*, Tahiti) and dissected. The gonado-visceral mass was fixed in 5% saline formalin, rinsed after two days, and preserved in 70% ethanol for posterior analyses. Because the gonads of pearl oysters are imbedded in the gonado-visceral mass, their contribution to the total volume was estimated as the relative surface area of gonad tissues on a sagittal slide (Fournier et al., 2012b; Moullac et al., 2013). We measured the surface area of gonads using images captured and digitalized at 300 dpi with a scanner (Epson Perfection 4990 Photo) and processed using Adobe

Photoshop (CS3) and ImageJ (v.1.51j8). The shell length (mean ± SD) of the animals used for estimating gonad-development index was 9.36 ± 0.89 cm (range = 6.20 – 12.20 cm).

2.3. Dynamic Energy Budget (DEB) model growth predictions

Rooted in the robust Dynamic Energy Budget (DEB) theory, DEB models allow quantification of the energy flow between the environment and an organism, and the dynamics of energy allocation towards reserves, structure (i.e., growth), maintenance, maturation, and reproduction (Kooijman, 2010; Sousa et al., 2010). For a detailed perspective of the DEB model structure and assumptions see Kooijman (2010) and Sousa et al. (2010). Here we highlight that DEB models can elegantly account for both the influence of changes in food availability and body temperature on energy fluxes (e.g., Monaco et al., 2014; Monaco and McQuaid, 2018; Troost et al., 2010). We used the most recently-parameterized DEB model for *P. margaritifera*, which was previously validated using populations from the Tuamotu and Gambier Archipelagoes (Sangare et al., 2020, 2019), to predict changes in shell length in response to the variability in seawater temperature and Chl-*a*. In this model, temperature affects the rates at which energy is allocated among physiological functions (e.g., growth) following a left-skewed thermal-performance curve (Fig. 2a). The parameter values that describe the curve were estimated by Sangare et al. (2020), considering long-term responses by the species (Sangare et al., 2020, 2019). The feeding process is described by a type-II functional response model, which predicts relative ingestion as a function of food availability (Fig. 2b). The standard form of this curve depends on the half-saturation coefficient parameter (X_κ), which defines the food level that yields 50% of the feeding capacity (0.2 μg Chl-*a* L^{-1} for *P. margaritifera*, Sangare et al., 2020). The model also includes the somatic maintenance rate, $[\dot{p}M]$, a parameter that defines the volume-specific energy expenditure of the individual (5.4 J cm^{-3} d^{-1} for *P. margaritifera*, Sangare et al., 2020). Departures from the species-specific $[\dot{p}M]$ values can indicate physiological stress (Pousse et al., 2019).

We used the DEB model, along with the daily measurements of temperature and Chl-*a* (see *2.1. Sampling location and environmental conditions*), to predict the growth of each of the 100 individuals measured for the empirical growth determination (see *2.2. Empirical observations of growth and reproduction*). Because each animal was measured on four occasions, we examined the

growth over time in three successive intervals. We began the simulations assuming the initial size of each animal at the beginning of each interval, while setting the reserves and reproduction state variables at maximum and mean-observed levels, respectively (Monaco and McQuaid, 2018; Sangare et al., 2020).

2.4. Data analyses

All data were analysed using R v3.6.2 (R Core Team, 2019).

We analysed the empirical growth data (shell length) for the 3 time intervals in two ways: based on the absolute rate of change (i.e., mm d^{-1}), and based on the specific growth rate (i.e., % d^{-1}). The former allowed comparing the observed values directly against those in the literature, while the latter is a more robust estimate for comparing growth among individuals of different initial lengths (Lugert et al., 2016). Animals were smaller than the asymptotic length reported for the species in French Polynesia (~15-30 cm; Coeroli et al., 1984). To test for the effect of time interval on growth rates and gonad-development index, we used the Kruskal-Wallis test (as data were non-parametric), followed by a Dunn test for multiple comparisons.

To estimate the model fit we used the mean absolute error (*MAE*), computed as the mean absolute difference between the empirical and predicted final shell lengths. We additionally tested the hypotheses that modifying both the feeding functional response curve and the somatic maintenance rate could further improve the model performance, and inform about unaccounted processes related to feeding (e.g., Alunno-Bruscia et al., 2011; Thomas and Bacher, 2018) and/or physiological stress (e.g., Pousse et al., 2019). Specifically, we ran 3 million additional simulations (100 individuals x 3 time intervals x 100 X_κ values x 100 $[\dot{p}M]$ values) allowing the half-saturation coefficient parameter (X_κ) to vary between 0 and 5 (0.05-unit intervals) µg Chl-*a* L^{-1}, and the volume-specific somatic maintenance rate ($[\dot{p}M]$) ranging between 0 and 20 (0.2-unit intervals) J cm^{-3} d^{-1}. The *best* values for X_κ and $[\dot{p}M]$ were judged based on the lowest *MAE*.

3. Results

3.1. Environmental variables

We found differences in environmental drivers across the time intervals considered, particularly regarding temperature dynamics (Fig. 3). Temperatures were highest and least variable during interval 1 (mean ± SD = 30.1 ± 0.5 °C). As temperature decreased gradually during interval 2, the mean was intermediate, but the variability was highest (mean ± SD = 27.8 ± 1.1 °C). Interval 3 was in turn the coolest, with intermediate variability (mean ± SD = 27.3 ± 0.6 °C).

While the mean Chl-*a* was comparable across time intervals, the variability increased progressively from interval 1 (mean ± SD = 0.766 ± 0.195 μg Chl-*a* L^{-1}) to interval 2 (mean ± SD = 0.919 ± 0.468 μg Chl-*a* L^{-1}) and interval 3 (mean ± SD = 0.943 ± 0.767 μg Chl-*a* L^{-1}) (Fig. 3).

3.2. Empirical observations of growth and reproduction

Time interval affected both estimates of empirical growth rate, absolute (Kruskal-Wallis test: df = 2, $\chi^2 = 38.15$, $p < 0.001$) and specific (df = 2, $\chi^2 = 39.91$, $p < 0.001$) (Figs. 4a and 4b). Individuals grew the fastest during interval 2, at intermediate level during interval 1, and the slowest during interval 3 (Dunn test: specific growth, $p < 0.05$ for all contrasts) (Fig. 4a). The mean (± SD) absolute shell growth was relatively low for the study location: 0.04 mm d^{-1} (± 0.05), 0.06 mm d^{-1} (± 0.05), and 0.01 mm d^{-1} (± 0.09) for intervals 1, 2, and 3, respectively (Fig. 4b). Mortality was negligible during the growth-measurement period (only one of the 100 individuals died).

As growth, the gonad-development index was relatively low for the region, with an overall mean (± SD) of 0.13 (± 0.11). Gonad-development index was higher during interval 1 (mean ± SD = 0.20 ± 0.11) than 2 (mean ± SD = 0.08 ± 0.07) (Kruskal-Wallis test: df = 1, $\chi^2 = 234.81$, $p < 0.001$) (Fig. 4b), suggesting a spawning event at the population scale.

3.3. Dynamic Energy Budget (DEB) model growth predictions

Mean (± SD) predicted absolute growth was 0.21 mm d^{-1} (± 0.02), 0.18 mm d^{-1} (± 0.01), and 0.16 mm d^{-1} (± 0.01) for intervals 1, 2, and 3, respectively. Compared to the empirical growth data, the model

overpredicted the final shell length of oysters for intervals 1 (*MAE* = 1.46 cm), 2 (*MAE* = 1.42 cm), and 3 (*MAE* = 1.34 cm) (Fig. 5). The overall *MAE* across intervals was 1.41 cm (Fig. 6).

Increasing the values of both the half-saturation coefficient parameter, X_κ, and the somatic-maintenance rate, $[\dot{p}M]$, improved the overall model fit, reaching the lowest *MAE* (0.42 cm) with X_κ = 0.56 µg Chl-*a* L^{-1} and $[\dot{p}M]$ = 9.70 J cm^{-3} d^{-1}. At higher values of both parameters, the model fit was relatively insensitive to changes in X_κ and $[\dot{p}M]$ (Fig. 6).

4. Discussion

We found that although temperature and total Chl-*a* in Takaroa appeared propitious for the physiological performance of *P. margaritifera* in 2019, individuals grew remarkably slowly and exhibited a relatively low reproductive effort, revealing an overall deteriorated energetic condition. The DEB model simulations suggested that the underlying cause could be associated with both individuals' inability to effectively consume the phytoplankton available in the water column, and augmented physiological-stress levels. The finding that organisms continued to invest energy towards reproduction supports the notion that energy allocation to growth and reproduction are not competing processes in *P. margaritifera*, as previously demonstrated both empirically and theoretically (Sousa et al., 2010). Ultimately, however, even if able to reproduce, the Takaroa population's recovery is unlikely if individual growth is limited.

4.1. Environmental drivers

Temperature varied seasonally across the duration of the study, with a particularly warm brief period (i.e., interval 1), and a protracted cooler period (intervals 2 and 3) (Fig. 3). The temperature amplitude was within those reported previously for the same lagoon (min–max, 26.0–30.5 ºC), and the neighbouring atolls of Takapoto (min–max, 25.7–30.4 ºC) and Manihi (min–max, 26.5–30.6 ºC) (Pouvreau and Prasil, 2001). Based on the thermal sensitivity of *P. margaritifera*, the thermal range at which energy fluxes are maximised is ~28–32 °C (Fig. 2). Accordingly, the relative thermal performance of individuals in Takaroa was consistently close to the optimal for the duration of our

study. Short-term thermal acclimation experiments suggest that temperatures above 30 ºC, as those we recorded during two months, are detrimental to the growth of *P. margaritifera* (Le Moullac et al., 2016). However, the thermal-sensitivity curve we used, which was fitted through the DEB parameter estimation protocol, integrates thermal responses across the whole life cycle of the organism (Kooijman, 2010; Sangare et al., 2020, 2019), and thus represents a more accurate measure characterization of the animals' thermal performance across periods longer than one or two weeks.

The mean values of food availability (i.e., total Chl-*a*) at Takaroa were stable across the 3 time intervals considered (Fig. 3), and considerably higher in 2019 than those reported previously for other locations. At Takapoto, a study that compiled mean measurements from 1974 to 1998 reported values ranging between 0.20 and 0.30 µg Chl-*a* L^{-1} (Delesalle et al., 2001). At the lagoon of Ahe, values from 2007 to 2010 ranged between 0.08 and 1.76 µg Chl-*a* L^{-1} (Charpy et al., 2012; Fournier et al., 2012b, 2012a; Thomas et al., 2010), and in 2013 between 0.30 and 0.80 µg Chl-*a* L^{-1} (Pagano et al., 2017). The temporal variability in our measurements, however, differed across time intervals (Fig. 3). The higher variability detected during intervals 2 and 3 reflects the recurrent presence of important peaks in Chl-*a* values, which we did not observe in interval 1.

4.2. Empirical observations of growth and reproduction

Our empirical observations showed that animals could grow and reproduce throughout the duration of the study (Fig. 4). Together with the observation that minimal mortalities were recorded during the study, this might suggest that individuals maintained a positive energy balance, presumably pointing to an auspicious population recovery (Sawusdee et al., 2015). However, relative to previous studies, the observed growth rate was extremely low. Based on the von Bertalanffy growth model estimates reported by Pouvreau and Prasil (2001) for the Takaroa and Takapoto Atolls, the expected growth rates of our animals were ~0.10 and ~0.09 mm d^{-1}, respectively, more than twice as fast as our observations (~0.04 mm d^{-1}). *In situ* measurements at Takapoto (Coeroli et al., 1984) and Ahe (Sangare et al., 2020) Atolls suggest growth rates ~0.09 mm d^{-1} for pearl oysters of similar size than ours. Our growth rate observations were even lower than the estimated ~0.08 mm d^{-1} reported for the lagoon of Vairao (Tahiti, French Polynesia), an area characterized by low primary production (Ky and

Le Moullac, 2017). These data revealed that, while individuals at Takaroa had a positive scope for growth, their energy budget was nevertheless strongly diminished.

The gonad-development index was lower (overall mean 0.13; Fig. 4b) than previously reported. For the oligotrophic lagoon of Vairao (Tahiti), the mean value was 0.15, ranging between 0.05 and 0.23 (Lacoste et al., 2014). Additionally, at the more productive lagoon of Ahe, which exhibits similar hydrobiological conditions to the Takaroa Lagoon, the mean gonad-development index was 0.17, ranging between 0.09 and 0.30 (Fournier et al., 2012b). The temporal variability in the gonad-development index showed two distinct periods during our observations; high reproductive potential before April and relatively low values thereafter. A similar trend was also documented by Fournier et al. (2012b), who found higher values (0.22) between January and April, followed by a period of lower gonad-development index (0.12) between April and July. This was attributed to a strong and synchronous spawning event associated with a decrease in phytoplankton availability (Fournier et al., 2012b). While we found no support for this relationship at Takaroa, as mean Chl-*a* did not change drastically across time intervals, the apparent spawning event we found between time intervals 1 and 2 further supports the idea that despite the energetic constraints, individual reproduction could be maintained.

The result that growth was relatively more affected than reproduction is particularly interesting because it shows that these processes need not to compete for available energy resources, as demonstrated empirically and theoretically for animals that exhibit indeterminate growth, including invertebrates, fishes, reptiles, and amphibians (Heino and Kaitala, 1999; Kozlowski, 1996). But to further understand why growth was more affected by the energy deficit than reproduction, it is necessary to consider the process of energy allocation quantitatively. DEB formulations explicitly remove the direct competition between these processes based on the κ-rule, where a fixed proportion of mobilized reserves (κ) is directed to growth and somatic maintenance, and the rest (1- κ) goes to reproduction and maturity maintenance (Kooijman, 2010; Sousa et al., 2010). The costs of somatic and maturity maintenance have priority over growth and reproduction, which is especially relevant if the energy mobilized from reserves becomes limited (Monaco et al., 2014). Because somatic

maintenance is substantially costlier than maturity maintenance in *P. margaritifera* (Sangare et al., 2020), its growth dynamics can be more sensitive to periods of reduced food availability than its reproductive capabilities (Monaco et al., 2014). This scenario is consistent with the different responses of growth and reproduction we found, and supports the notion that animals were indeed nutritionally deprived.

4.3. Perspective from the Dynamic Energy Budget (DEB) model

The question of how to reconcile the seemingly abundant food availability (total Chl-*a*) at Takaroa with the poor physiological condition in *P. margaritifera* individuals arises. A plausible explanation is that the available food was not accessible by the organisms, for example, due to unmet requirements of food particle size or nutritional quality (Dubois and Colombo, 2014; Ward and Shumway, 2004). The DEB model simulations, using *in situ* measurements of total Chl-*a* and temperature as drivers, allowed effectively testing this. By predicting faster growth than what was actually observed (Fig. 5), the original model (Sangare et al., 2020) suggested either limitations to the organism's feeding (i.e., energy provisioning) or increased maintenance costs associated with physiological stress (i.e., energy allocation). Minimizing the prediction error resulted in increases in the half-saturation coefficient by 1.8 fold and the somatic maintenance rate by 0.8 fold (Fig. 6), both being plausible explanations. Because tropical lagoons are characteristically poor in nutrients, *P. margaritifera* exhibits a low half-saturation coefficient that reflects its ability to profit from small increases in food, even at low phytoplankton concentration (Pouvreau et al., 1999). The higher new estimate of the half-saturation coefficient suggests a plastic response of the individual to adjust consumption of the microalgae species available. The current model implementation, however, for simplicity assumes that food availability is represented by total chlorophyll-*a*, and therefore cannot fully capture the complexities of the feeding process in the wild (Dubois and Colombo, 2014; Sarà et al., 2003; Ward and Shumway, 2004). The finding that somatic maintenance cost was also higher than for the generalized *P. margaritifera*, suggests the presence of an unknown stressor that reduced the physiological performance of individuals in Takaroa. For example, somatic maintenance can increase when bivalves are exposed to low salinity or microalgae-related toxins (Lavaud et al., 2017; Pousse et al., 2019).

To improve the DEB model's ability to describe variability in the ingestion/assimilation of food and somatic maintenance costs in *P. margaritifera*, further work is required in two axes: (1) adequate characterization of the trophic (e.g., type, size, nutritional value of food items) and physicochemical environment, and (2) restructuring the model to explicitly capture phenotypic plasticity in the feeding and maintenance components (Sangare et al., 2020). Regarding feeding, the literature, suggests that a likely culprit for the poor condition of *P. margaritifera* would be the dominance of picophytoplankton (i.e., microalgae 0.2–2-µm cell size) in the water column, which is too small for the organism to ingest (Loret et al., 2000; Pouvreau et al., 1999). Picophytoplankton cells have been associated with previous mass-mortality events in the region (Cabral, 1989), and their dominance over larger microalgae (i.e., nano and microphytoplankton) has increased over time in Takapoto (Delesalle et al., 2001). Similarly, the quality of the diet of filter feeders also depends on the inorganic content of the seston and the presence of non-chlorophyll-containing particles, some of which could be digested (Ward and Shumway, 2004). Microplastics, another form of non-chlorophyll-containing particles whose concentration is high in pearl-farming atolls, can in turn negatively affect the physiological condition of pearl oysters (Gardon et al., 2018). It is also possible that regardless of the food particle characteristics, the excess amount of food in Takaroa (as suggested by high total Chl-*a*) could have clogged the organism's cirri and labial palps, interfering with ingestion and assimilation (Chávez-Villalba et al., 2013). Regarding the augmented somatic maintenance, two conceivable drivers can be proposed for the Takaroa Atoll: microplastics and toxic algae, both of which can increase physiological stress (Gardon et al., 2018; Pousse et al., 2019).

Specific characteristics of the trophic and physicochemical environment can be accommodated into DEB models. For instance, for benthic filter-feeder species whose ingestion of carbon is dampened by the amount of inorganic matter in the water, the half-saturation coefficient is calculated based on both organic and inorganic particles in the water (Thomas and Bacher, 2018; Troost et al., 2010). Similarly, the dose-dependent toxic effects of microplastics or phytotoxins can be computed on the basis of a variable somatic maintenance rate parameter (Pousse et al., 2019). Similar developments could be implemented in the model of *P. margaritifera* to account for variation in food

type, including the presence of natural and exotic (e.g., microplastics; Gardon et al., 2018; Stamataki et al., 2020) inorganic matter, and toxic compounds in tropical lagoons. Resolving these components will improve the model's accuracy and broaden its scope (Sangare et al., 2020).

Finally, efforts that integrate the two working axes outlined above (i.e., characterizing the trophic and physicochemical environment and improving the DEB model structure) are essential. Comprehensive *in situ* descriptions of the environment is of course ideal. However, the remote nature and difficulty in accessing many pearl-farming atolls call for practical approaches that can produce data at high spatial and temporal resolution. While the rapid development of logging devices and remote-sensing technologies is currently satisfying much of the demand for environmental data, their estimates often depart significantly from the conditions truly experienced by the organism (Van Wynsberge et al., 2017, 2020). Chl-*a* concentration estimates from fluorescent probes, for instance, do not discriminate between the contribution of different phytoplankton groups, a development that would likely help to greatly improve the DEB model predictions for *P. margaritifera*. Ultimately, the accuracy and precision of this and other mechanistic models used across large and remote areas depends on innovations to our *in situ* and possibly remote-sensing technologies (Canonico et al., 2019).

4.4. Conclusion and future direction

Understanding the processes driving tropical marine mass-mortality events and the eventual recovery of populations is particularly challenging when diagnostic data are difficult to produce, as is the case for many Indo-pacific atolls and islands (Adjeroud et al., 2001; Cabral, 1989). Nevertheless, understanding their underlying mechanisms is necessary to improve the management practices of commercially-important and ecologically-relevant species, and to potentially prevent, or at least, anticipate, similar episodes in the future.

Our study demonstrates that the physiological condition of *P. margaritifera* in the Takaroa Atoll was suboptimal 5 years following a mass-mortality event, despite suitable temperatures and high food availability in the years that followed. This was confirmed empirically by the relatively poor

growth and reproduction, and by DEB model simulations which overpredicted the final size of animals raised in the lagoon. The apparent contradiction of having sufficient food but poor performance indicated that the model deviation could be explained by an inadequate handling of the feeding and physiological-stress processes by the predictive model. And finally, refitting the functional response curve by modifying the half-saturation coefficient and the somatic maintenance rate parameters demonstrated that a more nuanced formulation of these processes is needed for *P. margaritifera*, if we are to accurately capture the physiological mechanisms underlying their slow growth rate. By combining empirical evidence and the indirect inferences from DEB modelling, we can formally propose the hypotheses that the currently unknown characteristics of the phytoplankton community and physicochemical environment in Takaroa will delay the population's recovery.

Acknowledgements

This study was supported by the project Management of Atolls (MANA, ANR-16-CE32-0004). We thank the *Direction des ressources marines* (DRM, French Polynesia) for support, and especially V Liao for providing instruments and G Haumani for assisting during fieldwork. T Hauata (SCA QLES pearl farm) assisted with the collection of animals and hosted the research team at Takaroa.

5. References

Adjeroud, M., Andréfouët, S., Payri, C., 2001. Mass mortality of macrobenthic communities in the lagoon of Hikueru atoll (French Polynesia). Coral Reefs 19, 287–291. https://doi.org/10.1007/PL00006962

Alunno-Bruscia, M., Bourlès, Y., Maurer, D., Robert, S., Mazurié, J., Gangnery, A., Goulletquer, P., Pouvreau, S., 2011. A single bio-energetics growth and reproduction model for the oyster *Crassostrea gigas* in six Atlantic ecosystems. Journal of Sea Research 66, 340–348. https://doi.org/10.1016/j.seares.2011.07.008

Andréfouët, S., Charpy, L., Lo-Yat, A., Lo, C., 2012. Recent research for pearl oyster aquaculture management in French Polynesia. Marine Pollution Bulletin 65, 407–414. https://doi.org/10.1016/j.marpolbul.2012.06.021

Andréfouët, S., Dutheil, C., Menkes, C.E., Bador, M., Lengaigne, M., 2015. Mass mortality events in atoll lagoons: environmental control and increased future vulnerability. Global Change Biology 21, 195–205. https://doi.org/10.1111/gcb.12699

Andréfouët, S., Thomas, Y., Dumas, F., Lo, C., 2016. Revisiting wild stocks of black lip oyster *Pinctada margaritifera* in the Tuamotu Archipelago: The case of Ahe and Takaroa atolls and implications for the cultured pearl industry. Estuarine, Coastal and Shelf Science 182, 243–253. https://doi.org/10.1016/j.ecss.2016.06.013

Andréfouët, S., Genthon, P., Pelletier, B., Le Gendre, R., Friot, C., Smith, R., Liao, V., 2020. The lagoon geomorphology of pearl farming atolls in the Central Pacific Ocean revisited using detailed bathymetry data. Marine Pollution Bulletin 160, 111580. https://doi.org/10.1016/j.marpolbul.2020.111580

Beck, M.W., Brumbaugh, R.D., Airoldi, L., Carranza, A., Coen, L.D., Crawford, C., Defeo, O., Edgar, G.J., Hancock, B., Kay, M.C., Lenihan, H.S., Luckenbach, M.W., Toropova, C.L., Zhang, G., Guo, X., 2011. Oyster Reefs at Risk and Recommendations for Conservation, Restoration, and Management. BioScience 61, 107–116. https://doi.org/10.1525/bio.2011.61.2.5

Cabral, P., 1989. Some aspects of the abnormal mortalities of the pearl oysters, *Pinctada margaritifera* L. in the Tuamotu Archipelago. Aquacop IFREMER. Actes Colloq 9, 217–226.

Canonico, G., Buttigieg, P.L., Montes, E., Muller-Karger, F.E., Stepien, C., Wright, D., Benson, A., Helmuth, B., Costello, M., Sousa-Pinto, I., Saeedi, H., Newton, J., Appeltans, W., Bednaršek, N., Bodrossy, L., Best, B.D., Brandt, A., Goodwin, K.D., Iken, K., Marques, A.C., Miloslavich, P., Ostrowski, M., Turner, W., Achterberg, E.P., Barry, T., Defeo, O., Bigatti, G., Henry, L.-A., Ramiro-Sánchez, B., Durán, P., Morato, T., Roberts, J.M., García-Alegre, A., Cuadrado, M.S., Murton, B., 2019. Global Observational Needs and Resources for Marine Biodiversity. Frontiers in Marine Science 6, 367. https://doi.org/10.3389/fmars.2019.00367

Charpy, L., Rodier, M., Fournier, J., Langlade, M.-J., Gaertner-Mazouni, N., 2012. Physical and chemical control of the phytoplankton of Ahe lagoon, French Polynesia. Marine Pollution Bulletin 65, 471–477. https://doi.org/10.1016/j.marpolbul.2011.12.026

Chávez-Villalba, J., Soyez, C., Aurentz, H., Le Moullac, G., 2013. Physiological responses of female and male black-lip pearl oysters (*Pinctada margaritifera*) to different temperatures and concentrations of food. Aquatic Living Resources 26, 263–271. https://doi.org/10.1051/alr/2013059

Coeroli, M., Gajllande, D.D., Landret, J.P., 1984. Recent innovations in cultivation of molluscs in French Polynesia. Aquaculture 39, 45–67.

Delesalle, B., Sakka, A., Legendre, L., Pagès, J., Charpy, L., Loret, P., 2001. The phytoplankton of Takapoto Atoll (Tuamotu Archipelago, French Polynesia): time and space variability of biomass, primary production and composition over 24 years. Aquat. Living Resour. 8.

Dubois, S.F., Colombo, F., 2014. How picky can you be? Temporal variations in trophic niches of co-occurring suspension-feeding species. Food Webs 1, 1–9. https://doi.org/10.1016/j.fooweb.2014.07.001

Fournier, J., Dupuy, C., Bouvy, M., Couraudon-Réale, M., Charpy, L., Pouvreau, S., Le Moullac, G., Le Pennec, M., Cochard, J.-C., 2012a. Pearl oysters *Pinctada margaritifera* grazing on natural plankton in Ahe atoll lagoon (Tuamotu archipelago, French Polynesia). Marine Pollution Bulletin 65, 490–499.

Fournier, J., Levesque, E., Pouvreau, S., Pennec, M.L., Le Moullac, G., 2012b. Influence of plankton concentration on gametogenesis and spawning of the black lip pearl oyster *Pinctada margaritifera* in Ahe atoll lagoon (Tuamotu archipelago, French Polynesia). Marine Pollution Bulletin 65, 463–470. https://doi.org/10.1016/j.marpolbul.2012.03.027

Harris, P., Fichez, R., 1995. Observations et mécanismes de la crise dystrophique de 1994 dans le lagon de l'atoll d'Hikueru (Archipel des Tuamotu, Polynésie Française). ORSTOM, Notes et Documents Oceanographie, Tahiti 45.

Gardon, T., Reisser, C., Soyez, C., Quillien, V., Le Moullac, G., 2018. Microplastics affect energy balance and gametogenesis in the pearl oyster *Pinctada margaritifera*. Environmental Science & Technology 52, 5277–5286. https://doi.org/ 10.1021/acs.est.8b00168

Heino, M., Kaitala, V., 1999. Evolution of resource allocation between growth and reproduction in animals with indeterminate growth. Journal of Evolutionary Biology 12, 423–429.

Intes, A., 1995. The natural pearl shell populations in French Polynesia. SPC Pearl Oyster Information Bulletin 8, 17–24.

Jackson, J.B.C., 2008. Ecological extinction and evolution in the brave new ocean. Proceedings of the National Academy of Sciences 105, 11458–11465. https://doi.org/10.1073/pnas.0802812105

Keenan, E.E., Brainard, R.E., Basch, L.V., 2008. Historical and present status of the pearl oyster, *Pinctada margaritifera*, in the Northwestern Hawaiian Islands, in: Proceedings of the 11th International Coral Reef Symposium. Ft. Lauderdale, FL, USA, p. 12.

Kooijman, S.A.L.M., 2010. Dynamic Energy Budget Theory for Metabolic Organization, 3rd ed.

Kozlowski, J., 1996. Optimal allocation of resources explains interspecific life-history patterns in animals with indeterminate growth. Proc R Soc Lond B 263, 559–566.

Ky, C.-L., Le Moullac, G., 2017. Shell growth performance of hatchery produced *Pinctada margaritifera*: Family effect and relation with cultured pearl weight. Journal of Aquaculture Research and Development 8. https://doi.org/10.4172/2155-9546.1000480

Lacoste, E., Le Moullac, G., Levy, P., Gueguen, Y., Gaertner-Mazouni, N., 2014. Biofouling development and its effect on growth and reproduction of the farmed pearl oyster *Pinctada margaritifera*. Aquaculture 434, 18–26.

Lallias, D., Arzul, I., Heurtebise, S., Ferrand, S., Chollet, B., Robert, M., Beaumont, A.R., Boudry, P., Morga, B., Lapègue, S., 2008. *Bonamia ostreae* -induced mortalities in one-year old European flat oysters *Ostrea edulis*: experimental infection by cohabitation challenge. Aquat. Living Resour. 21, 423–439. https://doi.org/10.1051/alr:2008053

Lavaud, R., La Peyre, M.K., Casas, S.M., Bacher, C., La Peyre, J.F., 2017. Integrating the effects of salinity on the physiology of the eastern oyster, Crassostrea virginica, in the northern Gulf of Mexico through a Dynamic Energy Budget model. Ecological Modelling 363, 221–233. https://doi.org/10.1016/j.ecolmodel.2017.09.003

Le Moullac, G., Soyez, C., Latchere, O., Vidal-Dupiol, J., Fremery, J., Saulnier, D., Lo Yat, A., Belliard, C., Mazouni-Gaertner, N., Gueguen, Y., 2016. *Pinctada margaritifera* responses to temperature and pH: Acclimation capabilities and physiological limits. Estuarine, Coastal and Shelf Science 182, 261–269. https://doi.org/10.1016/j.ecss.2016.04.011

Loret, P., Pastoreaud, A., Bacher, C., Delesalle, B., 2000. Phytoplankton composition and selective feeding of the pearl oyster *Pinctada margaritifera* in the Takapoto lagoon (Tuamotu Archipelago, French Polynesia): in situ study using optical microscopy and HPLC pigment analysis. Mar. Ecol. Prog. Ser. 199, 55–67. https://doi.org/10.3354/meps199055

Lugert, V., Thaller, G., Tetens, J., Schulz, C., Krieter, J., 2016. A review on fish growth calculation: multiple functions in fish production and their specific application. Rev Aquacult 8, 30–42. https://doi.org/10.1111/raq.12071

McAfee, D., McLeod, I.M., Boström-Einarsson, L., Gillies, C.L., 2020. The value and opportunity of restoring Australia's lost rock oyster reefs. Restor Ecol 28, 304–314. https://doi.org/10.1111/rec.13125

Monaco, C.J., McQuaid, C.D., 2018. Applicability of Dynamic Energy Budget (DEB) models across steep environmental gradients. Scientific Reports 8, 16384. https://doi.org/10.1038/s41598-018-34786-w

Monaco, C.J., Wethey, D.S., Helmuth, B., 2014. A dynamic energy budget (DEB) model for the keystone predator *Pisaster ochraceus*. PLoS ONE 9, e104658. https://doi.org/10.1371/journal.pone.0104658

Moullac, G.L., Soyez, C., Sham-Koua, M., Levy, P., Moriceau, J., Vonau, V., Maihota, M., Cochard, J.C., 2013. Feeding the pearl oyster *Pinctada margaritifera* during reproductive conditioning. Aquaculture Research 44, 404–411. https://doi.org/10.1111/j.1365-2109.2011.03045.x

Nel, R., Cetzee, P., Van Niekerk, R., 1996. The evaluation of two treatments to reduce mud worm (*Polydora hoplura* Claparède) infestation in commercially reared oysters (*Crassostrea gigas* Thunberg). Aquaculture 141, 31–39.

Nielsen, P., Petersen, J.K., 2019. Flat oyster fishery management during a time with fluctuating population size. Aquat. Living Resour. 32, 22. https://doi.org/10.1051/alr/2019020

Pousse, É., Flye-Sainte-Marie, J., Alunno-Bruscia, M., Hégaret, H., Rannou, É., Pecquerie, L., Marques, G.M., Thomas, Y., Castrec, J., Fabioux, C., Long, M., Lassudrie, M., Hermabessiere, L., Amzil, Z., Soudant, P., Jean, F., 2019. Modelling paralytic shellfish toxins (PST) accumulation in *Crassostrea gigas* by using Dynamic Energy Budgets (DEB). Journal of Sea Research 143, 152–164. https://doi.org/10.1016/j.seares.2018.09.002

Pouvreau, S., Jonquières, G., Buestel, D., 1999. Filtration by the pearl oyster, *Pinctada margaritifera*, under conditions of low seston load and small particle size in a tropical lagoon habitat. Aquaculture 176, 295–314. https://doi.org/10.1016/S0044-8486(99)00102-7

Pouvreau, S., Prasil, V., 2001. Growth of the black-lip pearl oyster, *Pinctada margaritifera*, at nine culture sites of French Polynesia: synthesis of several sampling designs conducted between 1994 and 1999. Aquatic Living Resources 14, 155–163. https://doi.org/10.1016/S0990-7440(01)01120-2

R Core Team, 2019. R: A language and environment for statistical computing. R Foundation for Statistical Computing, Vienna, Austria.

Rodier, M., Longo, S., Henry, K., Ung, A., Lo-Yat, A., Darius, H., Viallon, J., Beker, B., Delesalle, B., Chinain, M., 2019. Diversity and toxic potential of algal bloom-forming species from Takaroa lagoon (Tuamotu, French Polynesia): a field and mesocosm study. Aquat. Microb. Ecol. 83, 15–34. https://doi.org/10.3354/ame01900

Samain, J.F., McCombie, H. (Eds.), 2008. Summer mortality of Pacific oyster *Crassostrea gigas*: the Morest project. Editions Quae.

Sangare, N., Lo-Yat, A., Le Moullac, G., Pecquerie, L., Thomas, Y., Beliaeff, B., Andréfouët, S., 2019. Estimation of physical and physiological performances of blacklip pearl oyster larvae in view of DEB modeling and recruitment assessment. Journal of Experimental Marine Biology and Ecology 512, 42–50. https://doi.org/10.1016/j.jembe.2018.12.008

Sangare, N., Lo-Yat, A., Moullac, G.L., Pecquerie, L., Thomas, Y., Lefebvre, S., Gendre, R.L., Beliaeff, B., Andréfouët, S., 2020. Impact of environmental variability on *Pinctada margaritifera* life-history traits: A full life cycle deb modeling approach. Ecological Modelling 423, 109006. https://doi.org/10.1016/j.ecolmodel.2020.109006

Sarà, G., Giommi, C., Giacoletti, A., Conti, E., Mulder, C., Mangano, M.C., 2021. Multiple climate-driven cascading ecosystem effects after the loss of a foundation species. Science of The Total Environment 770, 144749. https://doi.org/10.1016/j.scitotenv.2020.144749

Sarà, G., Vizzini, S., Mazzola, A., 2003. Sources of carbon and dietary habits of new Lessepsian entry Brachidontes pharaonis (Bivalvia, Mytilidae) in the western Mediterranean. Marine Biology 143, 713–722. https://doi.org/10.1007/s00227-003-1118-4

Sawusdee, A., Jensen, A.C., Collins, K.J., Hauton, C., 2015. Improvements in the physiological performance of European flat oysters *Ostrea edulis* (Linnaeus, 1758) cultured on elevated reef structures: Implications for oyster restoration. Aquaculture 444, 41–48. https://doi.org/10.1016/j.aquaculture.2015.03.022

Seuront, L., Nicastro, K.R., Zardi, G.I., Goberville, E., 2019. Decreased thermal tolerance under recurrent heat stress conditions explains summer mass mortality of the blue mussel Mytilus edulis. Sci Rep 9, 17498. https://doi.org/10.1038/s41598-019-53580-w

Sousa, T., Domingos, T., Poggiale, J.-C., Kooijman, S.A.L.M., 2010. Dynamic energy budget theory restores coherence in biology. Phil. Trans. R. Soc. B 365, 3413–3428. https://doi.org/10.1098/rstb.2010.0166

Stamataki, N., Hatzonikolakis, Y., Tsiaras, K., Tsangaris, C., Petihakis, G., Sofianos, S., Triantafyllou, G., 2020. Modelling mussel (*Mytilus spp.*) microplastic accumulation. Ocean Sci. 16, 927–949. https://doi.org/10.5194/os-16-927-2020

Thomas, Y., Bacher, C., 2018. Assessing the sensitivity of bivalve populations to global warming using an individual-based modelling approach. Global Change Biology 24, 4581–4597. https://doi.org/10.1111/gcb.14402

Thomas, Y., Garen, P., Courties, C., Charpy, L., 2010. Spatial and temporal variability of the pico- and nanophytoplankton and bacterioplankton in a deep Polynesian atoll lagoon. Aquat. Microb. Ecol. 59, 89–101. https://doi.org/10.3354/ame01384

Troost, T.A., Wijsman, J.W.M., Saraiva, S., Freitas, V., 2010. Modelling shellfish growth with dynamic energy budget models: an application for cockles and mussels in the Oosterschelde (southwest Netherlands). Philosophical Transactions of the Royal Society B: Biological Sciences 365, 3567–3577. https://doi.org/10.1098/rstb.2010.0074

Van Wynsberge, S., Menkes, C., Le Gendre, R., Passfield, T., Andréfouët, S., 2017. Are Sea Surface Temperature satellite measurements reliable proxies of lagoon temperature in the South Pacific? Estuarine, Coastal and Shelf Science 199, 117–124. https://doi.org/10.1016/j.ecss.2017.09.033

Van Wynsberge, S., Le Gendre, R., Sangare, N., Aucan, J., Menkes, C., Liao, V., Andréfouët, S., 2020. Monitoring pearl farming lagoon temperature with global high resolution satellite-derived products: An evaluation using Raroia Atoll, French Polynesia. Marine Pollution Bulletin 160, 111576. https://doi.org/10.1016/j.marpolbul.2020.111576

Ward, E.J., Shumway, S.E., 2004. Separating the grain from the chaff: particle selection in suspension- and deposit-feeding bivalves. Journal of Experimental Marine Biology and Ecology 300, 83–130. https://doi.org/10.1016/j.jembe.2004.03.002

Figure legends

Figure 1 Map of the Takaroa Atoll (Tuamotu Archipelago, French Polynesia), with our study location indicated with a black point. The inset shows the position of the atoll within the Pacific Ocean.

Figure 2 Dynamic Energy Budget model curves to describe the influence of (a) body temperature and (b) total chlorophyll-*a* (proxy for food availability) on the rates of energy allocation of *Pinctada margaritifera*. Parameter values that define the curves are from Sangare et al. (2020). Only the half-saturation coefficient (X_κ) is indicated (by an arrow), as this is the only parameter we examined in this study.

Figure 3 Seawater temperature (°C) and total chlorophyll-*a* (µg Chl-*a* L^{-1}) recorded in Takaroa during three consecutive time intervals (interval 1, black, 30/01/2019 - 24/04/2019; interval 2, orange, 24/04/2019 - 15/08/2019; interval 3, light blue, 15/08/2019 - 06/11/2019). Panels (a) and (b) show mean (± SD) daily values of temperature and chlorophyll-*a*, respectively. Panel (c) shows the overall mean (± SD) temperature and total chlorophyll-*a* for each time interval.

Figure 4 Empirical growth and reproductive output of *Pinctada margaritifera* maintained in Takaroa. (a) Specific and (b) absolute shell growth measured for 100 individuals during three consecutive time intervals (interval 1, black, 30/01/2019 - 24/04/2019; interval 2, orange, 24/04/2019 - 15/08/2019; interval 3, light blue, 15/08/2019 - 06/11/2019). (b) Gonado-somatic index measured weekly for 30 individuals between 12/02/2019 and 23/07/2019. Different letters above the boxplots indicate significant differences between time intervals (Kruskal-Wallis test, Dunn test for multiple comparisons, $\alpha = 0.05$). Boxes show the 25^{th} and 75^{th} percentiles, and horizontal lines the medians. The whiskers illustrate the extreme values that are within 1.5 times the interquartile range. Points represent outliers.

Figure 5 Dynamic Energy Budget model predictions of growth (shell length, cm) for 100 *Pinctada margaritifera* simulated for three consecutive time intervals (interval 1, black, 30/01/2019 - 24/04/2019; interval 2, orange, 24/04/2019 - 15/08/2019; interval 3, light blue, 15/08/2019 - 06/11/2019). The initial shell length for each individual was the ones of the animals used in the

empirical growth measurements. Lines illustrate model predictions. The box plots and points describe the empirical measurements. The components of the box plots are as in Fig. 4.

Figure 6 Overall mean absolute errors (*MAE*s) for 10000 Dynamic Energy Budget (DEB) model simulations of *Pinctada margaritifera* shell lengths. Each simulation was computed using a different value for the parameters half-saturation coefficient (X_κ, µg Chl-*a* L^{-1}), ranging between 0 and 5 (0.05-unit intervals) µg Chl-*a* L^{-1}, and the volume-specific somatic maintenance rate ($[\dot{p}M]$, J cm^{-3} d^{-1}) ranging between 0 and 20 (0.2-unit intervals) J cm^{-3} d^{-1}. The circle indicates the X_κ and $[\dot{p}M]$ combination used in the original DEB model (Sangare et al., 2020), and the triangle indicates the value that yields the lowest *MAE*. Cyan and red colours in the background represent low and high *MAE*s, respectively. Blue contour lines separate *MAE* bins of 0.15-cm widths.

Figure 1

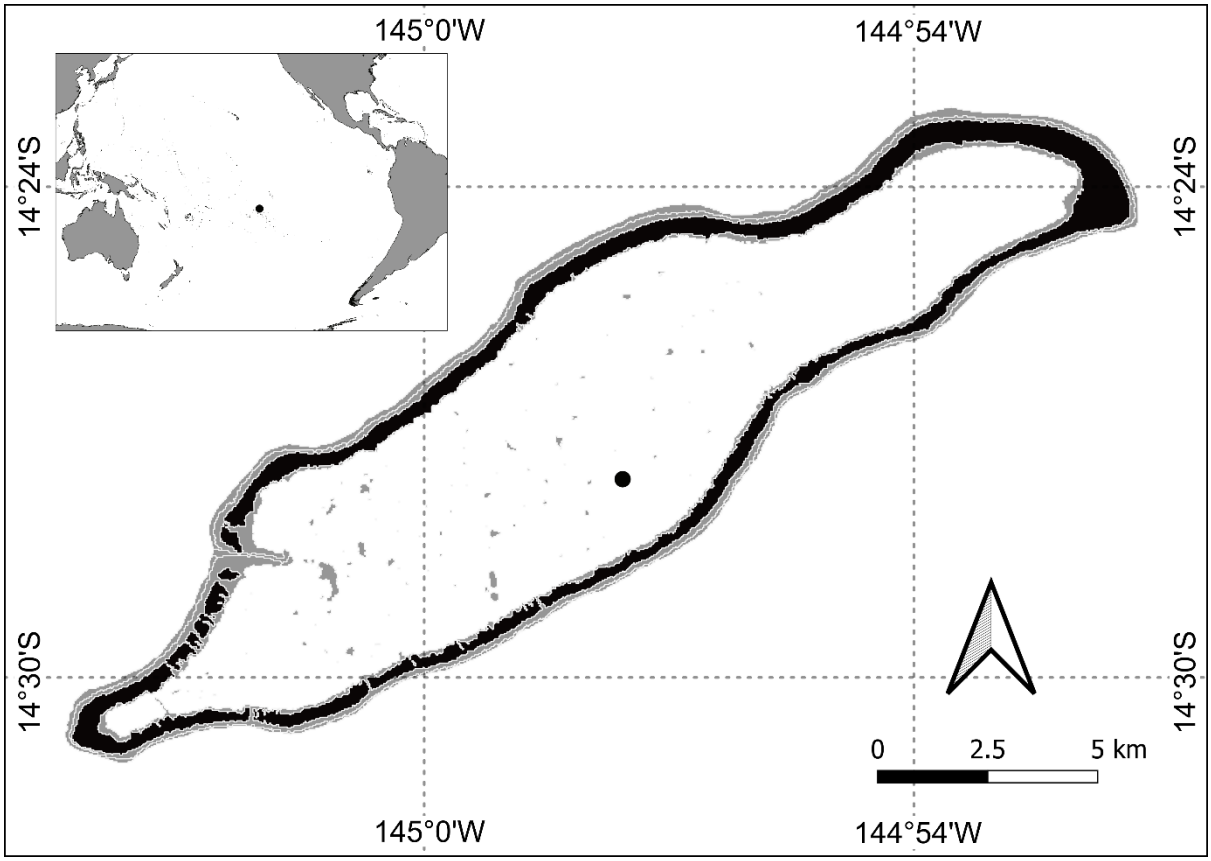

Figure 2

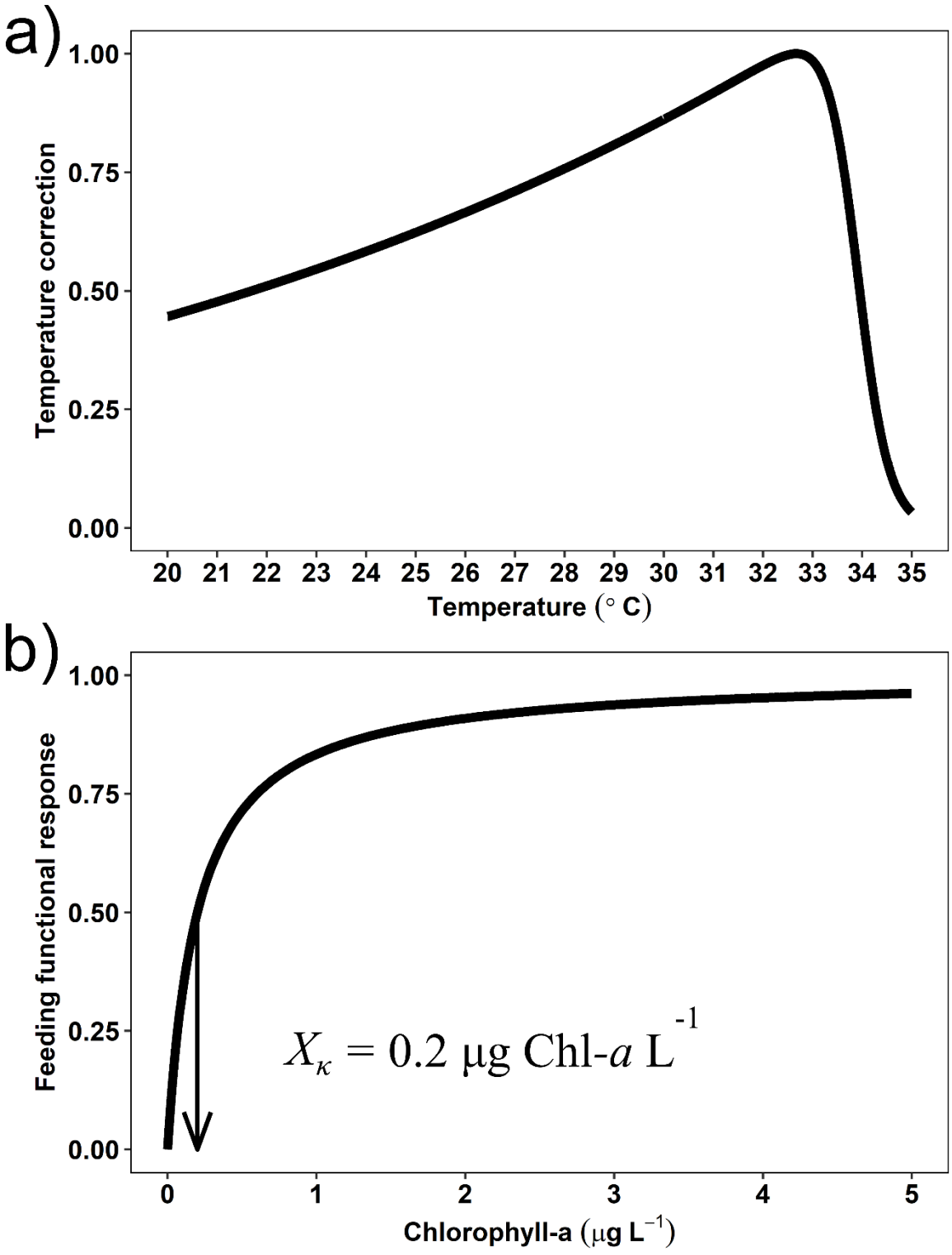
a)
1.00
0.75
0.50
0.25
0.00
Temperature correction
20 21 22 23 24 25 26 27 28 29 30 31 32 33 34 35
Temperature (° C)
b)
1.00
0.75
0.50
0.25
0.00
Feeding functional response
$X_\kappa = 0.2$ µg Chl-*a* L^{-1}
0 1 2 3 4 5
Chlorophyll-a (µg L^{-1})

Figure 3

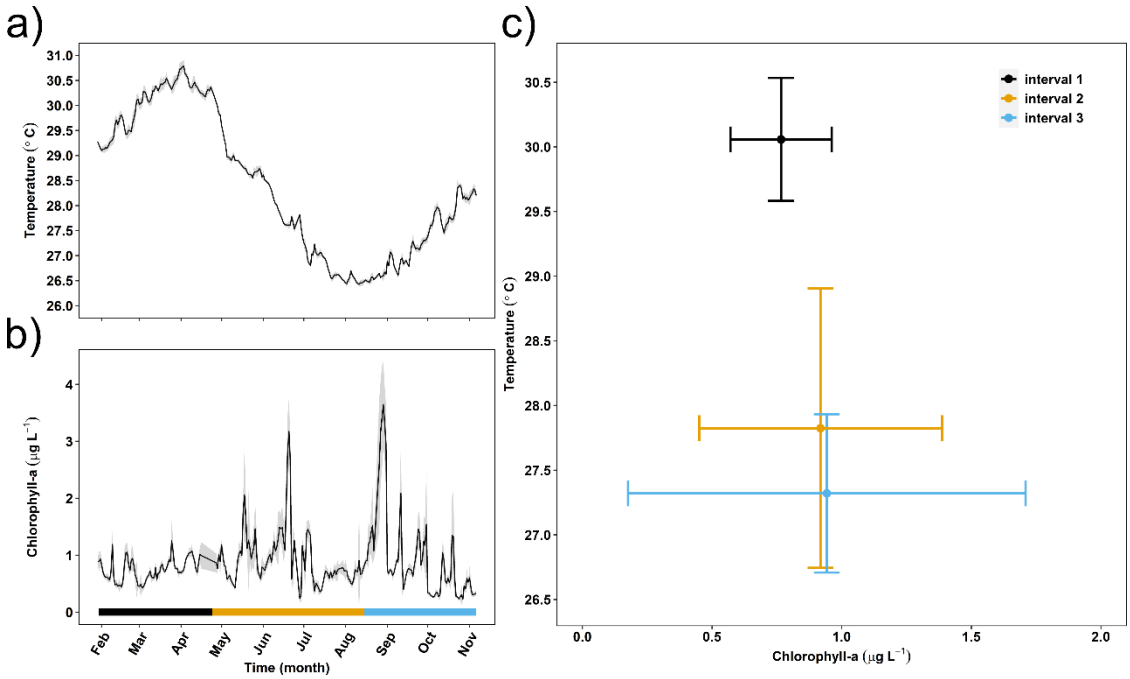
a)
b)
c)
Temperature (° C)
Chlorophyll-a (μg L⁻¹)
Time (month)
Feb
Mar
Apr
May
Jun
Jul
Aug
Sep
Oct
Nov
interval 1
interval 2
interval 3

Figure 4

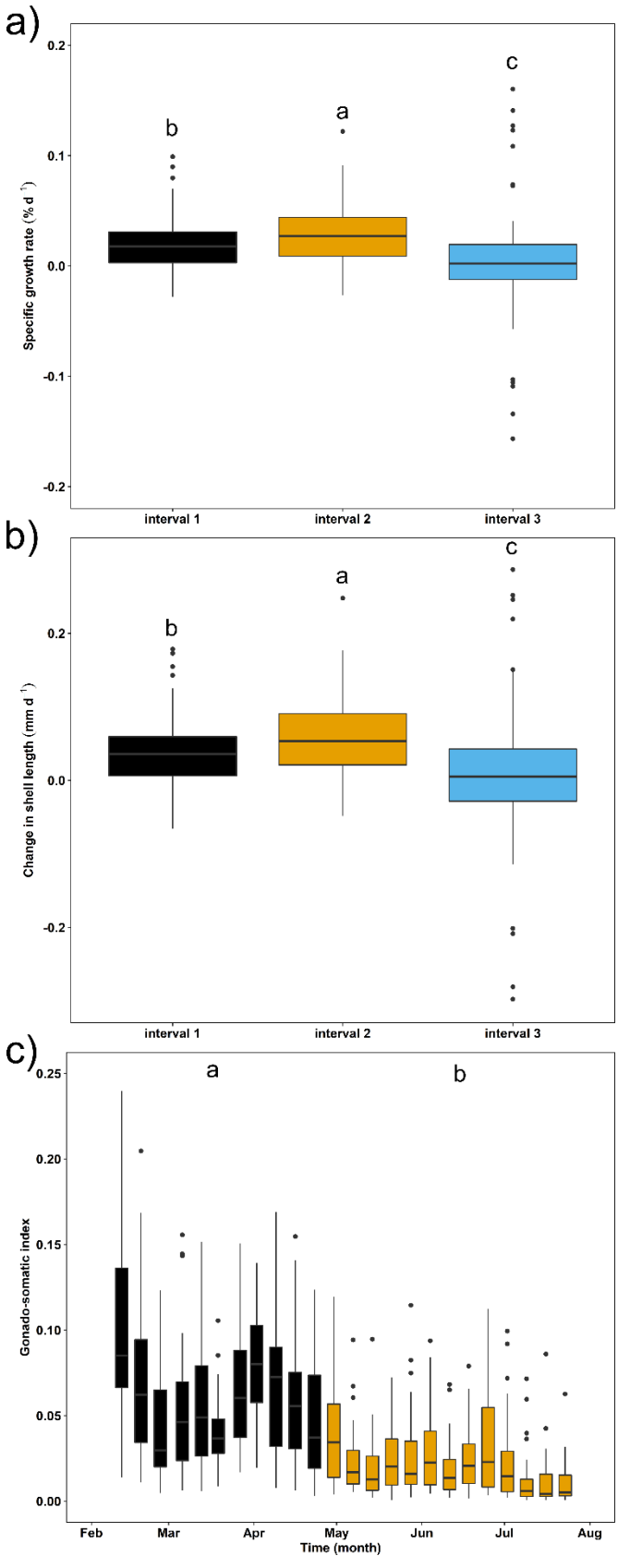
a)
Specific growth rate (% d⁻¹)
0.2
0.1
0.0
-0.1
-0.2
b
a
c
interval 1
interval 2
interval 3
b)
Change in shell length (mm d⁻¹)
0.2
0.0
-0.2
b
a
c
interval 1
interval 2
interval 3
c)
Gonado-somatic index
0.25
0.20
0.15
0.10
0.05
0.00
a
b
Feb
Mar
Apr
May
Jun
Jul
Aug
Time (month)

Figure 5

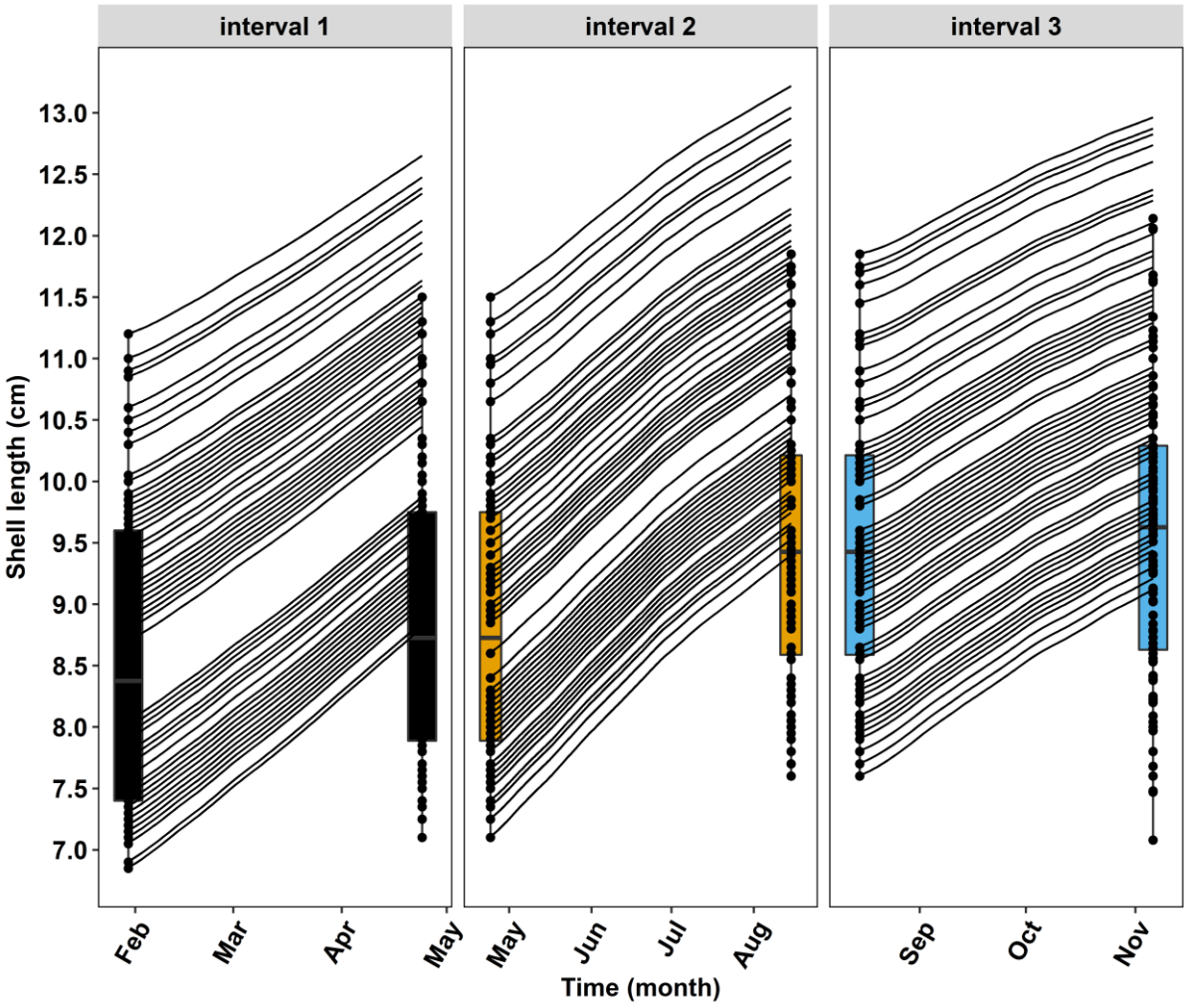
interval 1
interval 2
interval 3
Shell length (cm)
13.0
12.5
12.0
11.5
11.0
10.5
10.0
9.5
9.0
8.5
8.0
7.5
7.0
Feb
Mar
Apr
May
May
Jun
Jul
Aug
Sep
Oct
Nov
Time (month)

Figure 6

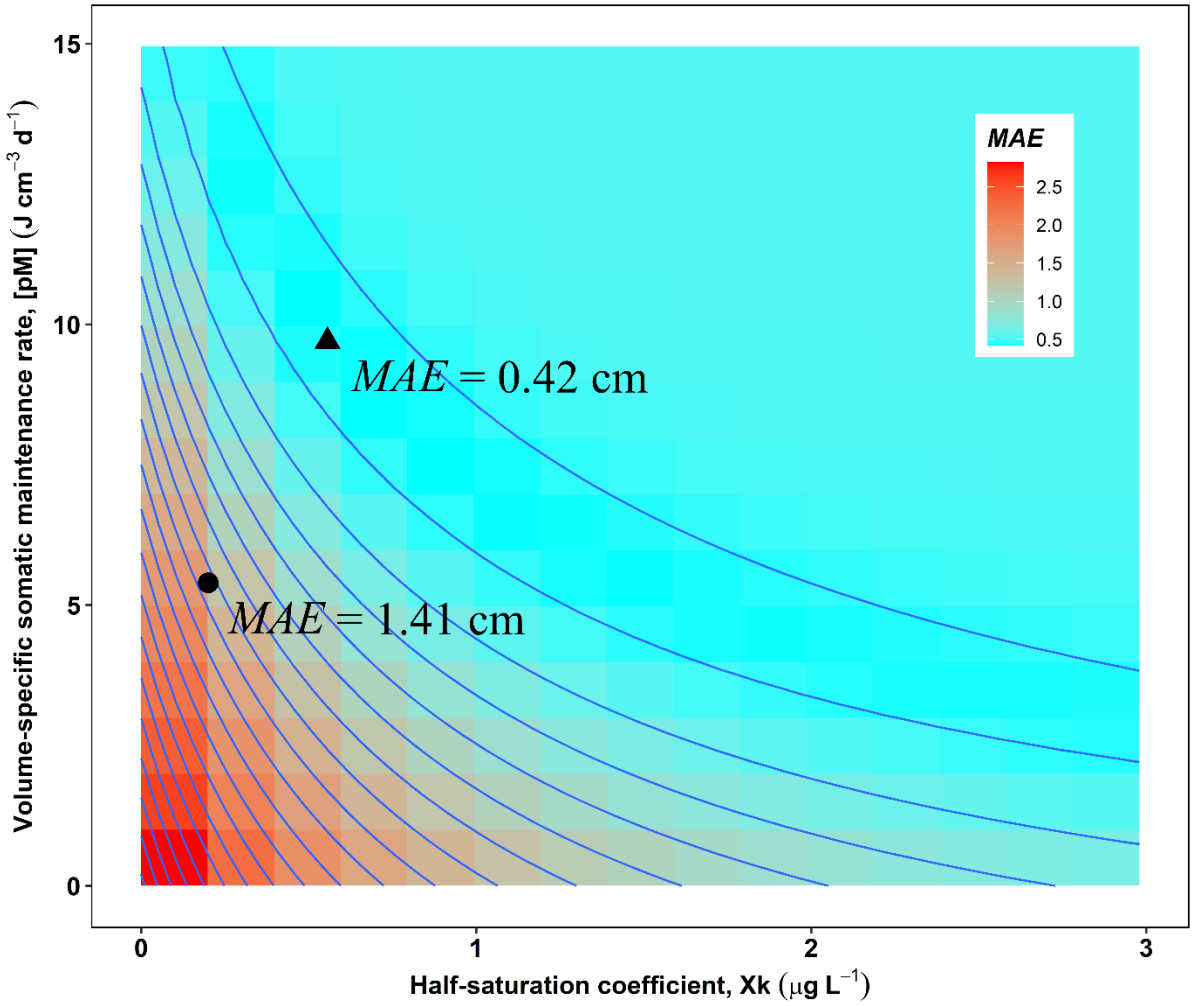
MAE
2.5
2.0
1.5
1.0
0.5
MAE = 0.42 cm
MAE = 1.41 cm
15
10
5
0
0
1
2
3
Volume-specific somatic maintenance rate, [pM] (J cm^{-3} d^{-1})
Half-saturation coefficient, Xk (μg L^{-1})